Trends in Renewable Energy
OPEN ACCESS ISSN: 2376-2144
Peer-Reviewed Article futureenergysp.com/index.php/tre

Double Carbon Coated $LiCoPO_4$ Nano Composite as High-Performance Cathode for Lithium Ion Batteries

Yong Yu[a], Huifang Zhao[a], Yao Chen[a], Zeng-kai Feng[b], Xiaomin Liu[a,*], and Hui Yang[a]

[a]*School of Material Science and Engineering, Nanjing Tech University, Nanjing, Jiangsu, China*
[b]*Foshan Branch, Beijing Landmark Engineering Co., Ltd., Foshan, Guangdong, China*

Received November 23, 2019; Accepted December 15, 2019; Published January 2, 2020

Polyacene(PAS)/carbon and acetylene black(AB)/carbon coated lithium cobalt phosphate composites were synthesized via the solid state reaction method using co-precipitated $Co_3(PO_4)_2 \cdot 8H_2O$ and Li_3PO_4 mixture as its precursor. X-ray powder diffraction (XRD) was performed to investigate the structure and phase of all the samples. The transmission electron microscopy (TEM) shows that the double carbon layers coated on the surface of $LiCoPO_4$ successfully. The $LiCoPO_4$/C, $LiCoPO_4$/PAS and $LiCoPO_4$/AB delivered a capacity of T 120.92, 121.07 and 138.06 $mAh \cdot g^{-1}$ at 0.1C, respectively. The double carbon coated $LiCoPO_4$ electrode delivered an initial discharge capacity of 147.12, 143.51 $mAh \cdot g^{-1}$ after AB/glucose, PAS/glucose coating, which maintained at 59.5% and 61.7% after 15 cycles at the 0.1C rate, respectively.

Keywords: Double carbon coated $LiCoPO_4$ nano composite; High-performance cathode; Lithium ion battery

Introduction

As renewable energy usage increases and price falls, energy storage becomes more and more important. The development of lithium-ion battery technology has opened the door to opportunities for the future of energy storage. For decades, scientists have been actively searching for new electrode materials and electrolytes that can produce a new generation of lithium-ion batteries which can provide greater energy storage, longer life, lower cost, and greater safety.

Olivine type $LiMPO_4$ (M = Fe, Mn, Co, Ni) cathode materials is one of the most promising positive electrode materials for next-generation lithium-ion batteries (LIBs) owing to the strong P-O covalent bond and the resulting stability [1]. Among $LiMPO_4$ materials, $LiFePO_4$ is widely applicated in the field of electric and hybrid electric vehicles (HEVs) [2, 3], because of its low cost, environmental benignity, excellent thermal stability and outstanding cyclability [4]. However, the energy density of $LiFePO_4$ (586 $Wh \cdot Kg^{-1}$) limits its further development due to the low discharge potential (3.4 V vs. Li^+/Li). $LiCoPO_4$ presents the Li^+ extraction/insertion behaviour at potentials around 4.8 V (vs. Li^+/Li), which is highly beneficial to its energy density (801 $Wh \cdot Kg^{-1}$). But its poor electronic conductivity (~10^{-9} $S \cdot cm^{-1}$) [5] and ion conductivity (8.8×10^{-8} $S \cdot cm^{-1}$ at 27°C) [6] make it difficult to exhibit Li^+ insertion/extraction. On the other hand, there is no suitable 5 V electrolyte matching with its high operating voltage, which is the essential

**Corresponding author:* liuxm@njtech.edu.cn

Tr Ren Energy, 2020, Vol.6, No.1, 1-11. doi: 10.17737/tre.2020.6.1.00108

reason for the fast capacity fading. Both causes lead to poor electrochemical performance and short service life of the pristine $LiCoPO_4$. In order to optimize the performance of $LiCoPO_4$, particle size reduction [7, 8], carbon coating [9-12] and cation doping on the Co site [13, 14] have been adopted to improve the initial discharge capacity and rate capability. The addition of conductive compounds or polymers can shrink the transport path length of Li ion, increase the electronic conductivity and modify the surface of pure $LiCoPO_4$ [15]. Moreover, a uniform and compact carbon network layer which can prevent direct contact between the active mass and HF in the electrolyte is critical for the cathode material.

In this paper, a novel double carbon layers coated $LiCoPO_4$ is designed, where carbon is the first layer to make the conductive carbon adhere tightly on the surface of $LiCoPO_4$, the polyacene (PAS) or acetylene black (AB) is the second layer coating on the inner carbon layer to enhance the electronic conductivity of $LiCoPO_4$. In addition, the outer carbon layer can prevent the spalling of the first carbon layer and avoid partial irreversible structure changes during its charging and discharging process, thus extending the cycle life.

Experimental

$LiCoPO_4$ samples were prepared by the solid-state sintering method, in which the precursors (Li_3PO_4 and $Co_3(PO_4)_2{\cdot}8H_2O$) were prepared via a co-precipitation route using a micro reactor followed by stirring at 60 ℃ for 1 h. The processing procedure of the precursor (Li_3PO_4 and $Co_3(PO_4)_2$) and bare $LiCoPO_4$ (LCP) were described in our previous paper [16].

For single carbon coated samples, the precursor LC-1 (n_{Li}:n_{Co} = 2:1 in the reactant) was mixed with 3 wt% acetylene black, 5 wt% phenol–formaldehyde resins or 10 wt% glucose using a planetary milling machine. The obtained mixture was calcined at 650 ℃ for 10h in an Ar/H_2 (5%) atmosphere to generate materials LCP/C, labelled as LCP/AB, LCP/PAS and LCP/C, respectively.

In order to get the double carbon coated $LiCoPO_4$ composites, the dried precursor was ball-milled with 10 wt% glucose for 5 h in ethanol. Then the samples were dried to evaporate ethanol and heated at 350 ℃ for 5 h to synthesize the glucose coated composites. The obtained composite was ball-milled with 1 wt% acetylene black for 5 h. Then the above mixture was calcined at 650 ℃ for 10 h in Ar/H_2 (5%) to generate LCP/C@AB. In the similar procedure, the LCP/C@PAS composites are obtained by substituting acetylene black with 3 wt% phenol–formaldehyde resin.

The crystal structure of synthesized materials was evaluated by powder X-ray diffraction (XRD, Model X'TRA, Thermo Electron, USA). The morphology and microstructure features were studied by using a field emission scanning electron microscope (FESEM, JSM-6700F, JEOL, Japan) and a transmission electron microscope (TEM, JEM-1010, JEOL, Japan).

For electrochemical performance testing, the cathode was prepared by coating a slurry of 7 active material, carbon black and PVDF with 75:15:10 wt% on aluminium foil, using N-methylpyrrolidone (NMP) as solvent, followed by vacuum-dried at 120℃ for 12h. The cathode electrode was characterized with CR2032 coin cells assembled in an argon-filled glove box. An electrochemical 2032 coin cell consisted of an active material as the cathode, lithium foil as the counter electrode, 1 M $LiPF_6$ in a 1:1 (by vol) mixture

of dimethyl carbonate (DMC) and ethylene carbonate (EC) as the electrolyte, and celgard 2400 as the separator. The galvanostatic cycling profiles of the cells were recorded at different current densities between 3.0 V-5.0 V under room temperature. The electrochemical impedance spectroscopy of these cells was also tested with an electrochemical workstation (CHI650D, Shanghai Chenhua Instrument Co., Ltd., China) in the frequency ranging from 0.1 Hz to 1 M Hz.

Results and Discussion

Fig.1 shows the XRD patterns of the LCP samples synthesized by using LC-1 as the precursor. Like LCP-1 in the previous study, the characteristic peaks of carbon and Li_3PO_4 were not detected in LCP/C, LCP/C@PAS and LCP/C@AB composite, all peaks were consistent with $LiCoPO_4$ [JCPDS#32-0552]. The refined lattice parameters and crystallite sizes for the as-obtained products are summarized in Table 1. The estimated crystallite size of LCP-1 is much larger than those of carbon coated samples, indicating that the carbon can prevent the growth of $LiCoPO_4$ particles efficiently. In addition, the parameters of LCP/C@PAS and LCP/C@AB are smaller than those of LCP/C, demonstrating that the growth of $LiCoPO_4$ crystallite is highly inhibited by residual carbon particles degraded from double carbon sources.

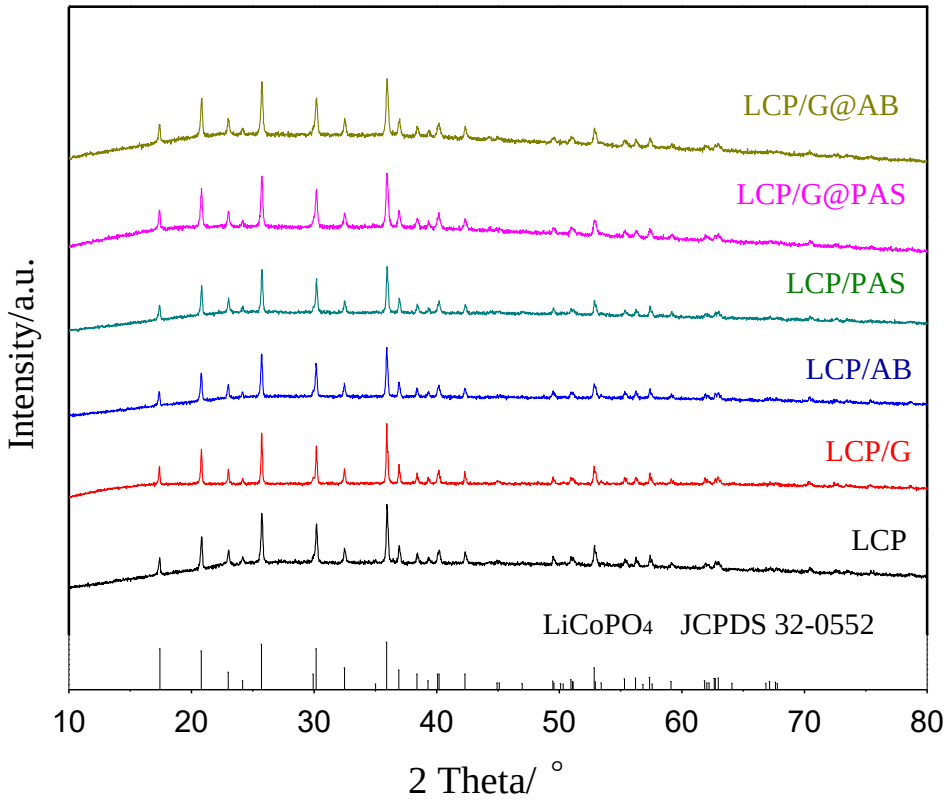

Fig. 1. XRD patterns of $LiCoPO_4$ composite samples

Table 1. The refined lattice parameters and crystallite sizes of LCP, LCP/C, LCP/G@PAS and LCP/G@AB

Sample name	A(Å)	b(Å)	c(Å)	V(Å)	Crystal size(nm)
LCP-1	5.9235	10.2132	4.7003	284.35	50.8796
LCP/C	10.2132	5.9235	4.7003	284.3582	49.8796
LCP/PAS	5.9235	10.2027	4.6992	283.99	48.8717
LCP/AB	10.2015	5.9131	4.6991	283.4614	47.9743
LCP/C@PAS	5.9274	10.1856	4.6220	279.05	41.3464
LCP/C@AB	5.9124	10.2026	4.6873	282.75	40.9086

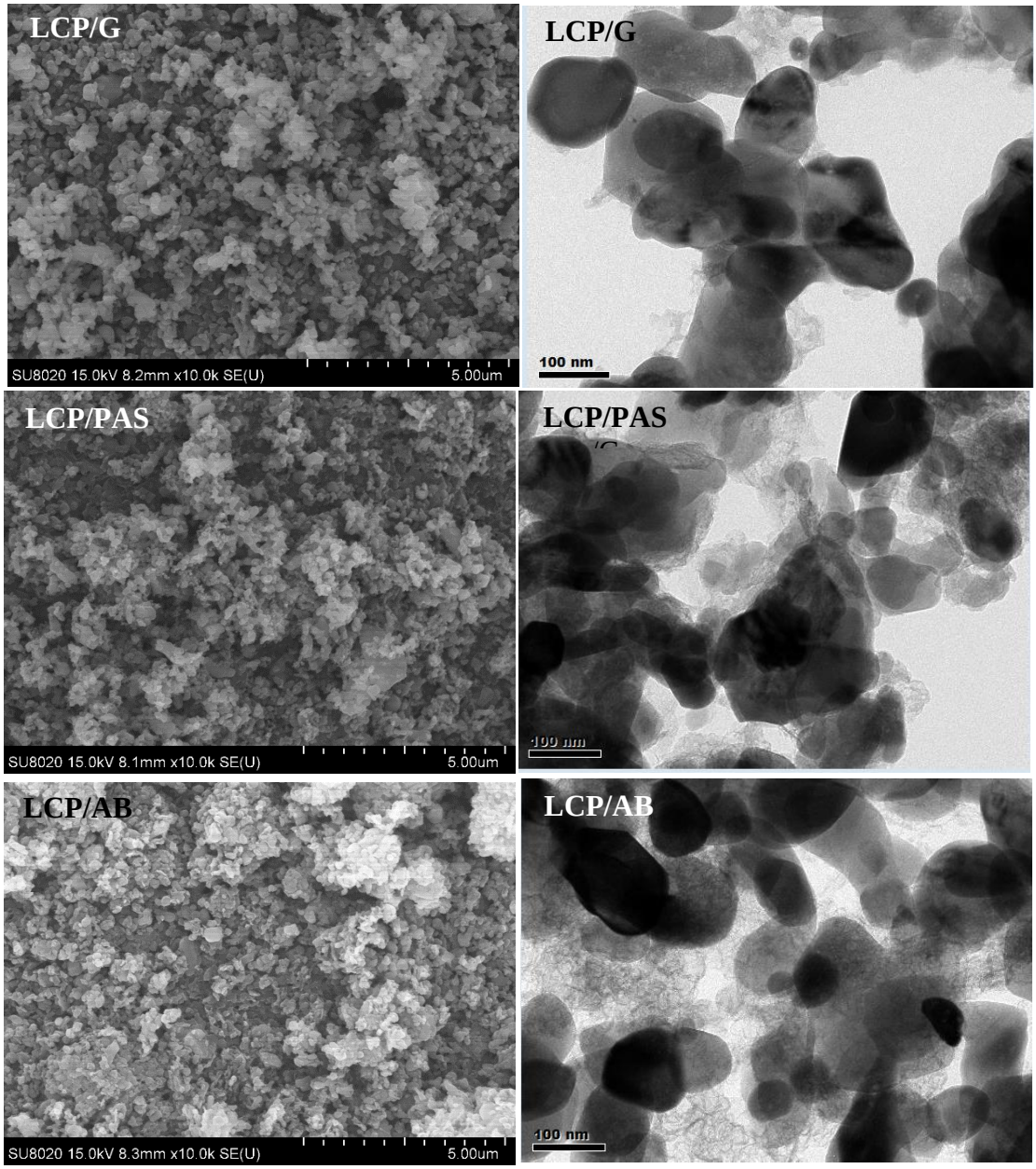

Fig. 2. SEM and TEM images of LCP/G, LCP/PAS and LCP/AB

The SEM and TEM images in Fig. 2 show the size, morphologies and carbon layer distribution of LCP/AB, LCP/C and LCP/PAS. The diameter scattering of LCP/G and LCP/PAS particles with slight agglomeration was uniform, in the range of 100-150 nm. The carbon pyrolyzed from organic glucose and phenol formaldehyde resin were different. For LCP/C, the carbon layer was coated on the $LiCoPO_4$ particles more tightly. The conductive polymer PAS layer had an increased thickness and presented a loose layer. Larger particles around 150 μm in size were formed in LCP/AB, and the floc-like pyrolytic products of acetylene black were dispersed among LCP particles, which may promote electronic conduction.

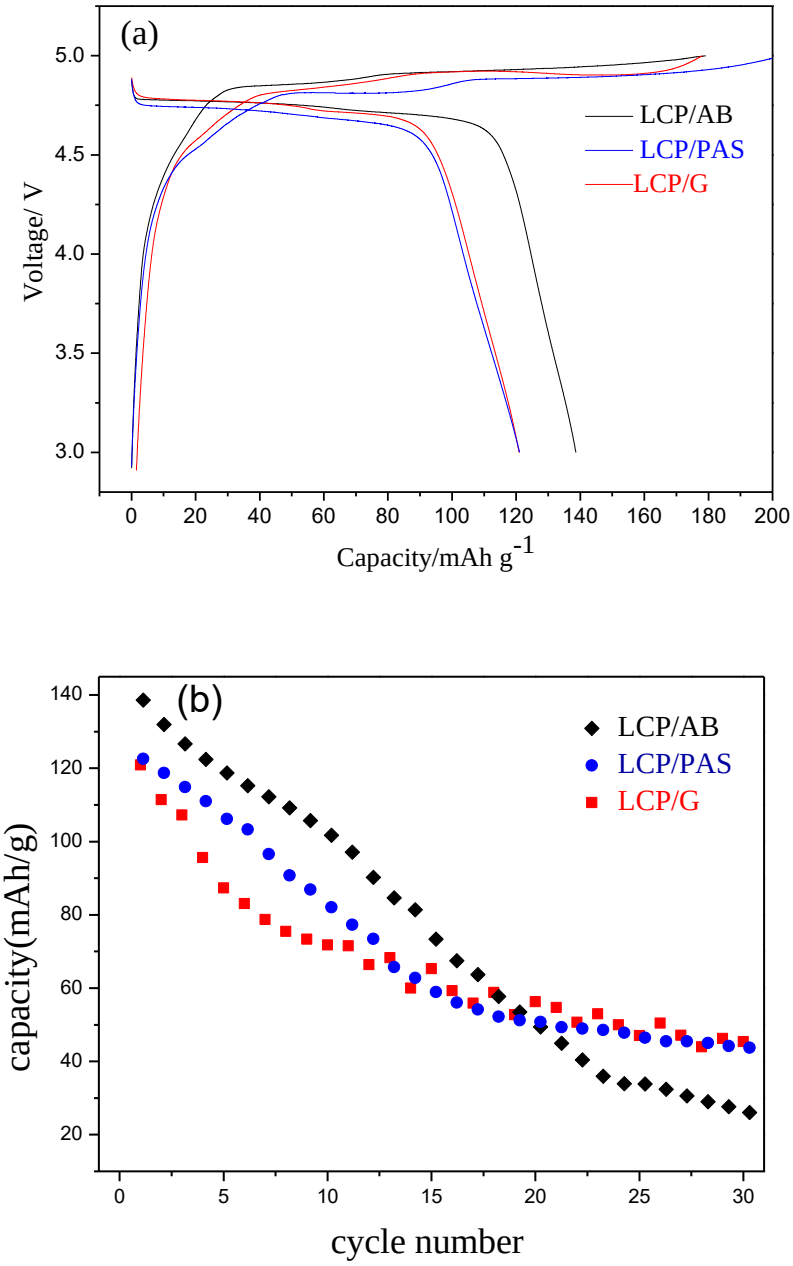

Fig. 3. Charge and discharge curves (a) and cycle performances of single carbon coated $LiCoPO_4$ composites at 0.1C (b)

Fig. 3 presents the electrical performance of single carbon coated $LiCoPO_4$ composites at 0.1C rate. Fig. 3a shows that the $LiCoPO_4$/C, $LiCoPO_4$/PAS, $LiCoPO_4$/AB owned a reversible capacity of 120.92, 121.07 and 138.06 mAh g^{-1}, respectively. Although LCP/AB presents the highest initial capacity, its capacity fading was very pronounced with a progressive decrease to 21.9 $mAh \cdot g^{-1}$ in the 30^{th} cycle. A better performance was achieved by glucose and phenol–formaldehyde resins pyrolytic carbonization. The LCP/G and LCP/PAS composites showed a similar capacity and capacity retention, which were 120.9 $mAh \cdot g^{-1}$, 3.7% and 121.1 $mAh \cdot g^{-1}$, 33.2%, respectively. The capacity curve of sample LCP/C dropped more sharply in the first 10 cycles. The carbon layer produced from pyrolysis of organic glucose and phenol–formaldehyde resins was more homogeneous and coated on the entire particle surface. The carbon decomposed by organic carbon, especially organic polymers was dispersed at the atomic level in the reaction system, which realized the uniform coating on the synthesized products and formed an interconnected conductive carbon film enhancing the structural stability, resulting in better cyclic performance.

Fig. 4 presents the TEM images of double carbon coated $LiCoPO_4$ samples. It is worth noting that the particle size of double carbon coated $LiCoPO_4$ was about 150 nm, which is smaller than those of LCP/C (200 nm on average). In the TEM photographs, it is found that the $LiCoPO_4$ particles were wrapped by two carbon layers. And the TEM images also exhibited the thickness and the boundary of the carbon layer on the surface of $LiCoPO_4$. The distribution of the carbon layer was related to the carbon source additives. In the case of LCP/C@PAS, the TEM images exhibited visually the $LiCoPO_4$ with hierarchical conductive architecture which consisted of 1.59 nm inner residual carbon layer and 1 nm outer polyacene polymer layer. But the outer polyacene layer distributeed unevenly. The sample LCP/C@AB presented a ~2 nm thick inner residual carbon layer and a 2.41 nm thick acetylene black outer layer. Although the carbon layer of LCP/C@AB was thicker than LCP/C@PAS, the outer layer was well-distributed.

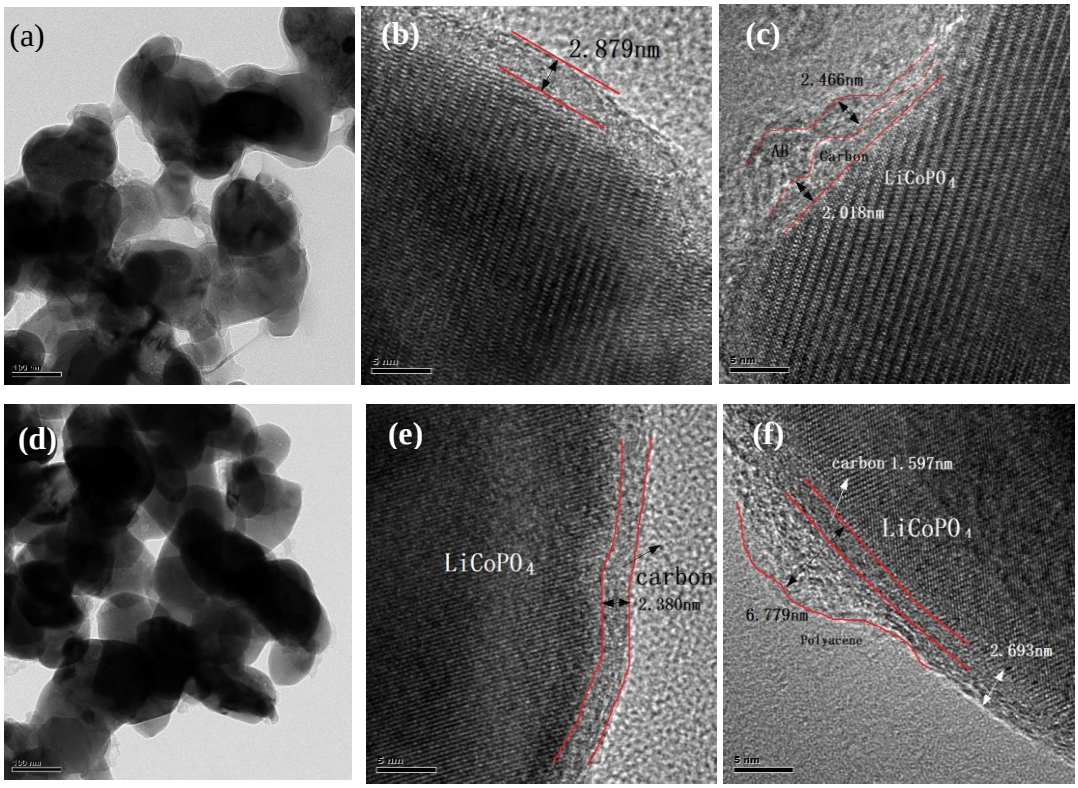

Fig. 4. TEM images of LCP/C@AB (a, b, c) and LCP/C@PAS (d,e,f)

The first charge and discharge curves of LCP/C@AB and LCP/C@PAS at 0.1C rate in the voltage of 3.0-5.0 V at room temperature are shown in Fig. 5. The second discharge capacity of LCP/C@PAS and LCP/C@AB were 134.79 and 138.78 $mAh \cdot g^{-1}$, respectively, which were higher than previous samples except LCP-3. All the charge curves displayed two obvious charge plateaus (one at about 4.8 V and the other at about 4.9 V) in the aspect of discharge profiles, and the quite different discharge behavior (shape of curve and evolution of voltage plateau) should be noted. A discharge plateau at ~4.8 V was obvious for LCP/C@PAS, while the LCP/C@AB showed a discharge plateau at 4.6 V. The discharge voltage of the active material fell sharply to the cut-off voltage (3.0 V), indicating a greater polarization. The LCP/C@AB exhibited a reversible specific capacity of 147.12 $mAh \cdot g^{-1}$ which was down to 59.5% and 11.9% after 15 cycles and 50 cycles, respectively. The LCP/C@PAS exhibited a reversible specific capacity of 143.51$mAh \cdot g^{-1}$ which was down to 61.7% after 15 cycles and remained up to 21.6% after 50 cycles. Compared with the samples of LCP/G, LCP/AB, LCP/PAS and LCP/G@AB, LCP/G@PAS showed a much better cyclability, which are mainly attributed to the synergistic effect of double carbon. On the one hand, the double carbon can more uniformly and finely refine the crystal particles, thereby shortening the length of the lithium ion transmission path, increasing the conductivity and modifying the surface of $LiCoPO_4$. On the other hand, the outer carbon layer can make the inner carbon layer more closely contact the active material, prevent the active material from directly contacting HF in the electrolyte, and prevent the inner layer from spalling during the charge and discharge process.

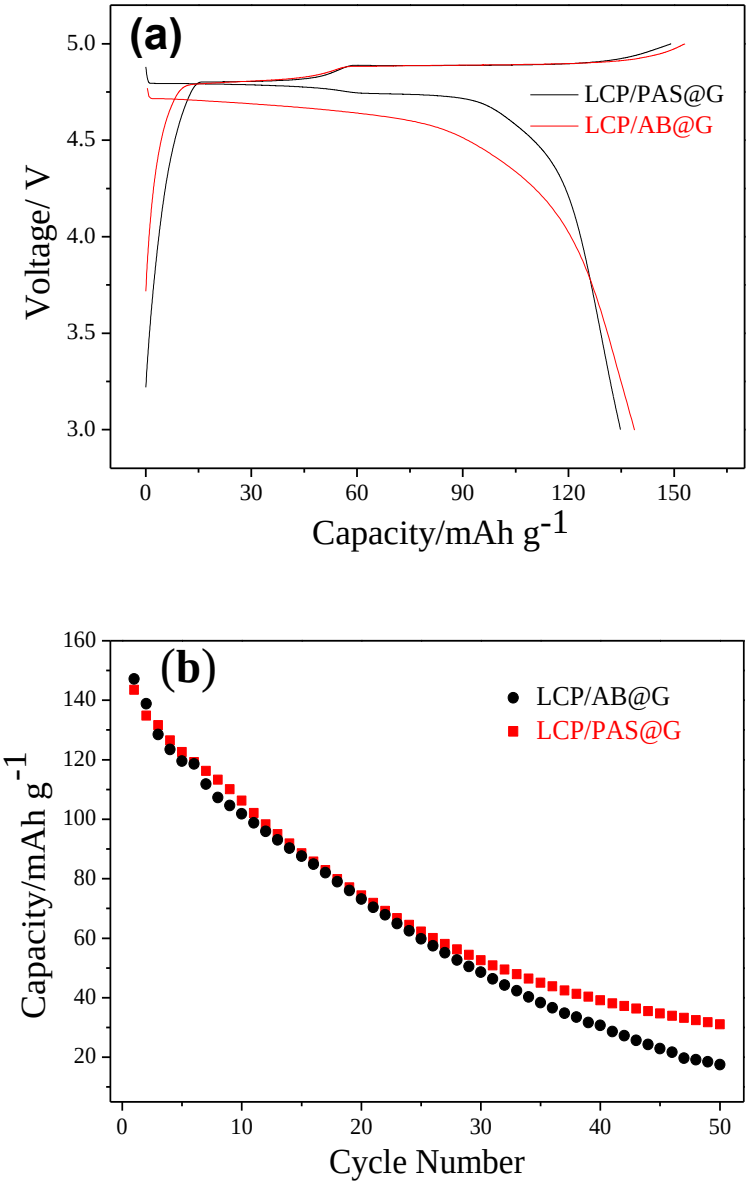

Fig. 5. Charge and discharge curves of double carbon coated $LiCoPO_4$ composite (a); Cycle performances of double carbon coated $LiCoPO_4$ composite at 0.1C (b)

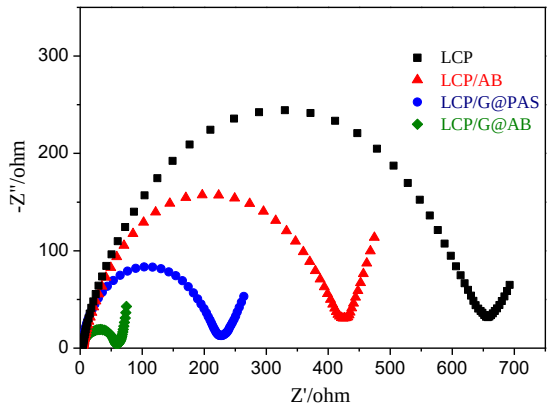

Fig. 6. Nyquist plots of the cells using $LiCoPO_4$ samples synthetized with different carbon sources.

Fig.6 presents the EIS impedance curves of the LCP and LCP/AB and double carbon coated samples $LiCoPO_4$/G@PAS and $LiCoPO_4$/G@AB at fully charged state after one cycle. The total impedance of the sample was mainly induced by the charge-transfer impedance between the electrolyte and the electrode interface, which could be assigned by the diameter of the semicircle in the curve. The diameter of the semicircle of the double carbon coated $LiCoPO_4$ was significantly smaller than that of pure LCP and single carbon coated LCP, and the impedance of the sample LCP/G@AB is the smallest. The small charge-transfer impedance of LCP/G@AB is attributed to the finer particles and the more stable architecture of double conducting layers, which benefits to its electrochemistry property distinctly, in accordance with its larger capacity.

CONCLUSIONS

In summary, the pyrolytic carbon coated $LiCoPO_4$ composites were synthesized by a micro-reactor assisted co-precipitation and then through a single/double carbon source coating route. $LiCoPO_4$/AB presented the largest initial discharge capacity of 138.06 $mAh \cdot g^{-1}$ among all single carbon coated $LiCoPO_4$ samples which could ascribe to the floc-like acetylene distributed in the LCP particles, thereby ameliorating the conductivity. And the discharge capacity and cyclability were further improved by glucose/AB and glucose/PAS coating, with initial capacities of 147.12 and 143.51 $mAh \cdot g^{-1}$, respectively. The longer cycle life of the $LiCoPO_4$/G@PAS sample can be ascribed to the finer particles and the more stable architecture of double conducting layers. The facile routine reported herein may be extended to prolong the cycle life of other electrode materials.

ACKNOWLEDGMENTS

This work was supported by the Natural Science Foundation of China (Grant No. 21573109), and the Priority Academic Program Development of Jiangsu Higher Education Institutions.

CONFLICTS OF INTEREST

The authors declare that there is no conflict of interests regarding the publication of this paper.

REFERENCES

[1] Truong, Q. D., Devaraju, M. K., Ganbe, Y., Tomai, T., and Honma, I. (2014). Controlling the shape of $LiCoPO_4$ nanocrystals by supercritical fluid process for enhanced energy storage properties. *Scientific Reports*, 4(2), 3975.

[2] Liu, X., Yan, P., Xie, Y., Yang, H., Shen, X. and Ma, Z. (2013) Synthesis of superior fast charging–discharging nano-$LiFePO_4$/C from nano-$FePO_4$ generated using a confined area impinging jet reactor approach, *Chemical Communication*, 49, 5396.

[3] Yan, P., Lu, L., Liu, X., Cao, Y., Zhang, Z., Yang, H. and Shen, X. (2013) An economic and scalable approach to synthesize high power $LiFePO_4$/C nanocomposites from nano-$FePO_4$ precipitated from an impinging jet reactor, *Journal of Materials Chemistry A*, 1, 10429

[4] Goodenough, J. B., and Park, K. S. (2013). The Li-Ion Rechargeable Battery: A Perspective. *Journal of the American Chemical Society*, 135(4), 1167-1176.

[5] Wolfenstine, J., Lee, U., Poese, B., and Allen, J. L. (2005). Effect of oxygen partial pressure on the discharge capacity of LiCoPO4. *Journal of Power Sources*, 144(1), 226-230. DOI: 10.1016/j.jpowsour.2004.12.013

[6] Morgan, D., Van der Ven, A., and Ceder, G. (2004). Li conductivity in LixMPO4 (M = Mn, Fe, Co, Ni) olivine materials. *Electrochemical and Solid State Letters*, 7(2), A30-A32. DOI: 10.1149/1.1633511

[7] Gangulibabu, Nallathamby, K., Meyrick, D., and Minakshi, M. (2013). Carbonate anion controlled growth of LiCoPO4/C nanorods and its improved electrochemical behavior. *Electrochimica Acta*, 101, 18-26. DOI: 10.1016/j.electacta.2012.09.115

[8] Wang, F., Yang, J., NuLi, Y., and Wang, J. (2011). Novel hedgehog-like 5V LiCoPO4 positive electrode material for rechargeable lithium battery. *Journal of Power Sources*, 196(10), 4806-4810. DOI: 10.1016/j.jpowsour.2011.01.055

[9] Liu, J., Conry, T. E., Song, X., Yang, L., Doeff, M. M., and Richardson, T. J. (2011). Spherical nanoporous LiCoPO4/C composites as high performance cathode materials for rechargeable lithium-ion batteries. *Journal of Materials Chemistry*, 21(27), 9984-9987. DOI: 10.1039/c1jm10793c

[10] Laszczynski, N., Birrozzi, A., Maranski, K., Copley, M., Schuster, M. E., and Passerini, S. (2016). Effect of coatings on the green electrode processing and cycling behaviour of LiCoPO4. *Journal of Materials Chemistry A*, 4(43), 17121-17128. DOI: 10.1039/c6ta05262b

[11] Wolfenstine, J., Read, J., and Allen, J. L. (2007). Effect of carbon on the electronic conductivity and discharge capacity LiCoPO4. *Journal of Power Sources*, 163(2), 1070-1073. DOI: 10.1016/j.jpowsour.2006.10.010

[12] The Nam Long, D., and Taniguchi, I. (2011). Preparation of LiCoPO4/C nanocomposite cathode of lithium batteries with high rate performance. *Journal of Power Sources*, 196(13), 5679-5684. DOI: 10.1016/j.jpowsour.2011.02.039

[13] Di Lecce, D., Manzi, J., Vitucci, F. M., De Bonis, A., Panero, S., and Brutti, S. (2015). Effect of the iron doping in LiCoPO4 cathode materials for lithium cells. *Electrochimica Acta*, 185, 17-27. DOI: 10.1016/j.electacta.2015.10.107

[14] Yang, S. M. G., Aravindan, V., Cho, W. I., Chang, D. R., Kim, H. S., and Lee, Y. S. (2012). Realizing the Performance of LiCoPO4 Cathodes by Fe Substitution with Off-Stoichiometry. *Journal of the Electrochemical Society*, 159(7), A1013-A1018. DOI: 10.1149/2.051207jes

[15] Ni, J., Wang, H., Gao, L., and Lu, L. (2012). A high-performance LiCoPO4/C core/shell composite for Li-ion batteries. *Electrochimica Acta*, 70, 349-354. DOI: 10.1016/j.electacta.2012.03.080

[16] Zhao, H., Yu, Y., Wang, G., Chen, Y., Liu, X., and Yang, H. (2018). Synthesis of nanosphere-like LiCoPO4 with excellent electrochemical performance via micro reactor assisted co-precipitation method. *Functional Materials Letters*, 11(05), 1850037. DOI: 10.1142/s1793604718500376